Article

Not peer-reviewed version

Molecular Mechanism of *OsSUT2* Regulating Chalkiness Formation in Rice Grains

Dongping Yao [†], Xiaoqiao Yin [†], Dengkui Liu, Fudie Meng, Chunfen Long, Yingge Li, Xuemei Zhong, Bin Bai [*]

Posted Date: 2 April 2026

doi: 10.20944/preprints202604.0166.v1

Keywords: rice; *OsSUT2* gene; chalkiness formation; sucrose transport; starch synthesis

 doi:10.20944/preprints202604.0166.v1

Article

Molecular Mechanism of *OsSUT2* Regulating Chalkiness Formation in Rice Grains

Dongping Yao [1,†], Xiaoqiao Yin [2,3,†], Dengkui Liu [1], Fudie Meng [2], Chunfen Long [2], Yingge Li [4], Xuemei Zhong [1] and Bin Bai [2,*]

[1] College of Plant Science and Technology, Hunan Biological and Electromechanical Polytechnic, Changsha, Hunan 410127, China

[2] State Key Laboratory of Hybrid Rice, Hunan Hybrid Rice Research Center, Changsha, Hunan 410125, China

[3] College of Life Sciences, Hunan Normal University, Changsha, 410081, China

[4] Hunan Yuanchuang Seed Industry Co., Ltd., Changsha, Hunan, 410323, China

* Correspondence: baibin87@163.com

[†] These authors have contributed equally to this work and share first authorship.

Abstract

Rice chalkiness is a key constraint on high-quality rice breeding, and unbalanced sucrose transport and starch metabolism are its primary causes. To clarify the molecular mechanism by which *OsSUT2* regulates rice grain chalkiness formation, the rice cultivar TP309 was used as material, and *ossut2* homozygous mutants were generated via CRISPR/Cas9. Systematic studies were performed using gene overexpression complementation, phenotypic identification, cytological observation, transcriptome sequencing and haplotype analysis. Results showed that loss of *OsSUT2* function significantly increased grain chalkiness, deteriorated agronomic traits, induced carbon assimilate accumulation in leaves, blocked sugar transport and starch synthesis in grains, and destroyed starch fine structure; normal phenotype was fully restored by *OsSUT2* overexpression. *OsSUT2* was expressed in both source and sink organs, with the most obvious inhibition detected in panicles. Mutation of *OsSUT2* disordered sucrose and starch metabolic pathways. Three main haplotypes of *OsSUT2* were identified in natural populations, with significant indica–japonica differentiation. *OsSUT2* is confirmed as a key regulator of rice chalkiness, providing gene resources and theoretical support for rice quality improvement.

Keywords: rice; *OsSUT2* gene; chalkiness formation; sucrose transport; starch synthesis

1. Introduction

Rice (*Oryza sativa L.*) is the primary staple food crop in China, and its yield and quality are inextricably linked to national food security [1]. With the escalation of consumer demands, rice chalkiness has emerged as a pivotal bottleneck hampering the breeding of high-quality rice cultivars in China. Chalkiness is defined as the white opaque regions in the endosperm, which are formed by the loose arrangement of starch granules and protein bodies during the grain filling stage; this structural abnormality markedly elevates the broken rice rate and impairs both the eating quality and commercial value of rice [2]. Although several genes associated with chalkiness, such as *Chalk5* and *WCR1*, have been characterized, chalkiness is a typical quantitative trait governed by multiple genes, and numerous key components of its intricate genetic regulatory network remain to be fully elucidated.

Starch and sucrose metabolism constitutes the core pathway for the accumulation of storage substances in rice endosperm, and the transmembrane transport and allocation of sucrose are mainly mediated by monosaccharide transporters (MSTs), sucrose transporters (SUTs) and sugar efflux transporters (SWEETs)[3]. Among the five identified members of the *OsSUT* family in rice with well-differentiated biological functions, *OsSUT2* is specifically localized to the tonoplast, where it mediates

 doi:10.20944/preprints202604.0166.v1

the transport of sucrose from the vacuole to the cytoplasm and is thus involved in the allocation of carbon assimilates between source and sink organs in rice plants [4–7]. Previous studies have demonstrated that *OsSUT2* cooperatively regulates carbohydrate transport with *GFD1* and *OsSWEET4*, thereby exerting an effect on grain filling. However, whether *OsSUT2* is directly involved in rice chalkiness formation remains unreported [8].

In recent years, considerable progress has been made in elucidating the regulatory mechanisms underlying rice chalkiness formation. The overexpression of *Chalk*5 disrupts the pH homeostasis of the endomembrane system, which in turn induces abnormal structures of protein bodies and impairs the arrangement of starch granules in the endosperm, ultimately modulating chalkiness formation [9]. Different alleles of the *Wx* gene influence the chalkiness phenotype by regulating the amylose content [10]. *WCR1*, a gene encoding an F-box protein, acts as a negative regulator of rice chalkiness; it stabilizes the MT2b protein through a dual mechanism, and then inhibits the core chalkiness rate in rice by enhancing reactive oxygen species (ROS) scavenging and delaying the programmed cell death (PCD) process in the endosperm [11]. The transcription factor NF-YB1 can directly regulate the expression of *OsSUT1*, *OsSUT3* and *OsSUT4*, thereby coordinately modulating grain filling and chalkiness formation [12]. In addition, functional defects of starch synthases (e.g., SSIIIa, BEIIb), debranching enzymes (e.g., ISA, PUL) and pentatricopeptide repeat (PPR) family proteins all lead to endosperm floury texture or increased chalkiness [13,14]. The research team led by Wan Jianmin has recently identified *OsTPS8* as a key gene associated with chalkiness, which encodes a trehalose-6-phosphate synthase. This protein interacts with *OsTPS1* to reduce the trehalose-6-phosphate (Tre6P) level, and then activates α-amylase to promote starch degradation, ultimately resulting in chalkiness formation. Natural variations in the promoter region of *OsTPS8* can be differentially regulated by the transcription factor *OsbHLH001*, thereby synergistically affecting rice chalkiness and seed vigor [15]. However, the role of vacuolar membrane sucrose transporters in chalkiness regulation has not been investigated to date, and this research gap limits a comprehensive understanding of the molecular network governing rice chalkiness formation.

In our preliminary work, we generated rice *OsSUT2* loss-of-function mutants *ossut2-1* and *ossut2-2* via the CRISPR/Cas9 genome editing technology, both of which exhibited a chalky phenotype characterized by severe ventral chalkiness, reduced starch accumulation and decreased 1000-grain weight. In the present study, we further systematically elucidate the biological function and molecular mechanism of *OsSUT2* in regulating rice chalkiness formation by integrating quality trait analysis, fine structural characterization and interactive protein screening, aiming to provide theoretical support and genetic resources for the breeding of high-quality rice cultivars.

2. Materials and Methods

2.1. Plant Materials and Cultivation Arrangements

In this study, rice cultivar Taipei 309 (TP309) was used as the wild-type control, and the *OsSUT2* gene (LOC_Os12g10840) was targeted for editing via the CRISPR/Cas9 gene editing technology to generate heritable chalky mutants *ossut2* with stable genetic traits. Sequencing validation revealed two types of mutants, namely *ossut2-1* (with a 54-bp deletion in the coding region) and *ossut2*-2 (with a 4-bp deletion in the coding region), both of which were homozygous mutants at the T3 generation. In addition, an overexpression vector of *OsSUT2* was constructed and introduced into the *ossut2-1* mutants via agrobacterium-mediated genetic transformation to obtain transgenic positive plants. All experimental materials were cultivated at the Transgenic Experimental Base in Changsha of Hunan Biological and Electromechanical Polytechnic and the Southern Breeding Base in Hainan. Conventional rice cultivation and management practices were adopted, with unified water and fertilizer regimes as well as consistent pest and disease control measures applied throughout the growth period.

 doi:10.20944/preprints202604.0166.v1

2.2. Determination of Agronomic Traits and Physicochemical Indices

At the mature stage, rice plants with consistent growth performance were selected to investigate agronomic traits including effective tiller number, total grains per panicle, 1000-grain weight, grain length and grain width. For each material, at least 10 plants were measured, and the average value was calculated. The chalkiness rate, chalkiness degree, total starch content, protein content and amylose content, as well as starch extraction, were determined according to our previously established method [16,17]. At the 20 days after flowering (DAF) during the grain filling stage, endosperms of wild-type TP309 and ossut2 mutant rice were sampled to determine the activities of soluble starch synthase (SSS), granule-bound starch synthase (GBSS), starch branching enzyme (SBE), debranching enzyme (DBE) and α-amylase (α-AL). For the assay of SSS and GBSS activities, crude enzyme extracts were prepared via ice-bath homogenization, and the enzyme activities were calculated by detecting the production of NADPH at a wavelength of 340 nm. The activity of SBE was characterized by the percentage decrease in absorbance of the starch-iodine complex at 660 nm. For DBE and α-AL, 3,5-dinitrosalicylic acid method was adopted, and their activities were determined by measuring the production of reducing sugars at 540 nm. A control tube was set for each enzyme activity assay, and the enzyme activity units were calculated on the basis of fresh weight or protein concentration [18,19].

The contents of glucose, fructose and sucrose in rice endosperms at the mature stage were determined by high-performance liquid chromatography (HPLC). The samples were subjected to ultrasonic extraction, followed by centrifugation and membrane filtration, and then detected using a Shimadzu LC-20AT HPLC system. For the samples at 20 DAF during the grain filling stage, the contents of the aforementioned sugars were measured by a micro biochemical method, and the content of Tre6p was determined using an ELISA kit. All indices were pretreated and detected according to the corresponding methods, and their contents were subsequently calculated.

2.3. Cytological Observation

Mature seeds of the wild-type and mutant lines were transversely sectioned at the middle part, and the sections were subjected to glutaraldehyde fixation, gradient dehydration, critical point drying and gold sputtering. The arrangement pattern, morphological characteristics and intergranular spacing of starch granules in the endosperm were then observed under a scanning electron microscope (SEM). In addition, the morphological features of the isolated starch granules were also examined via SEM (Philips XL-3, The Netherlands)[20].

2.4. Crystal Structure and Starch Chain-Length Distribution

The crystal structure of starch was analyzed via X-ray diffraction (XRD), and the crystallinity was calculated according to our previously established method [16]. Fourier transform infrared (FT-IR) spectroscopy was performed following the method described by Zhang's method [21]; the absorbance ratios of 1045/1022 cm^{-1} and 1022/995 cm^{-1} were determined to analyze the short-range order and intermolecular hydrogen bond strength of starch. The starch chain-length distribution was assayed by gel permeation chromatography-refractive index detection (GPC-RI) using a gel permeation chromatography-refractive index system. The liquid chromatography system was a U3000 (Thermo, USA) coupled with an OPTILAB T-rex refractive index detector (Wyatt Technology, CA, USA). Briefly, 5 mg of purified starch was dissolved in a boiling water bath and debranched with isoamylase in a water bath at 37 °C for 3 h, followed by precipitation with anhydrous ethanol. The precipitate was then redissolved in a DMSO/LiBr solution in a water bath at 80 °C for 2 h. Separation was carried out on a series of gel exclusion chromatography columns (Ohpak SB-805 HQ/803 HQ) with 0.5% LiBr-DMSO as the mobile phase, at a column temperature of 60 °C and a flow rate of 0.3 mL/min for gradient elution over 120 min. A standard curve was plotted using pullulan standards, and the chromatographic data were analyzed with ASTRA 6.1 software to obtain the characteristic starch chain-length distribution.

 doi:10.20944/preprints202604.0166.v1

2.5. Vector Construction and Genetic Transformation

An overexpression vector of *OsSUT2*, pBWA(V)KS-*OsSUT2*, harboring the double 35S promoter (eukaryotic G418-resistant) was constructed. Following validation by restriction enzyme digestion and Sanger sequencing, the recombinant plasmid was transformed into Agrobacterium tumefaciens strain EHA105. The calli of *ossut2-1* mutants were then transformed via Agrobacterium-mediated genetic transformation method. Transgenic plants were obtained through resistance screening, callus differentiation and rooting. Genomic DNA was extracted by the CTAB method, and positive transgenic lines were identified by PCR, thus completing the functional validation of *OsSUT2* overexpression.

2.6. Analysis of Gene Expression Patterns

2.6.1. Tissue-Specific Expression Analysis

Roots, stems, leaves, leaf sheaths, and panicles at 20 days after flowering (DAF) were sampled from TP309, *ossut2-1*, *ossut2*-2 rice plants. Total RNA was extracted using an RNA extraction kit, and complementary DNA (cDNA) was synthesized via reverse transcription. With the rice *UBIQUITIN* gene as the internal reference, the relative expression level of the *OsSUT2* gene was detected by reverse transcription quantitative real-time PCR (RT-qPCR). Three biological replicates were set for each sample, and the expression level was calculated using the $2^{-}\Delta\Delta Ct$ method.

2.6.2. Transcriptome Sequencing Analysis

Endosperm tissues of the wild-type and *ossut2* mutant lines at 20 days after flowering were sampled, with three biological replicates set for each genotype. Transcriptome sequencing was performed on the Illumina NovaSeq 6000 platform, and the experiment was conducted by Beijing Novogene Bioinformatics Technology Co., Ltd. After filtering the raw sequencing data, the clean reads were mapped to the rice reference genome (MSU7.0). Differentially expressed genes (DEGs) were screened using the DESeq2 software with the criteria of $|\log_2 FC| > 1$ and padj < 0.05, followed by Gene Ontology (GO) and Kyoto Encyclopedia of Genes and Genomes (KEGG) functional enrichment analyses. RT-qPCR validation was performed on the key DEGs to confirm the reliability of the transcriptome sequencing results.

2.7. Haplotype Analysis

To dissect the natural genetic diversity of the *OsSUT2* gene, a total of 6048 rice accessions from a natural population were retrieved from the RiceAtlas database [22] (http://60.30.67.242:18076/#/home). The coding region and flanking sequences of *OsSUT2* were subjected to sequencing and analysis, and haplotype classification was performed based on the combination characteristics of single nucleotide polymorphism (SNP) loci in the sequences. Furthermore, the distribution characteristics and indica-japonica differentiation pattern of the *OsSUT2* haplotypes were analyzed by integrating the indica-japonica classification information and geographical distribution data of the rice accessions.

2.8. Statistical Analysis

The analysis of all data was performed using the SPSS 24.0 statistical software program (IBM Corporation, Armonk, New York). One-way analysis of variance and Tukey's tests were used to determine whether statistically significant differences ($p < 0.05$) existed among the means. Bar charts were generated using Microsoft Excel and Graphpad Prism 10.1.2.

 doi:10.20944/preprints202604.0166.v1

3. Results and Disscussion

3.1. Phenotypic and Physicochemical Analysis of the Rice Chalkiness Mutant Ossut2

3.1.1. Isolation and Identification of the Ossut2 Mutants

The *OsSUT2* gene, located on chromosome 12 of the wild-type rice TP309 (WT), was targeted for editing using the CRISPR/Cas9 system. The target sequence selected was GCTGCCGCAGTTCTCACCGT. Through gene editing, T3 homozygous mutant lines exhibiting increased grain chalkiness were obtained. Sequencing analysis revealed two distinct mutation types in the coding region of *OsSUT2*: a 54-bp deletion and a 4-bp deletion. The line carrying the 54-bp deletion was designated *ossut2-1*, and the line with the 4-bp deletion was named *ossut2*-2 (Figure 1A–D).

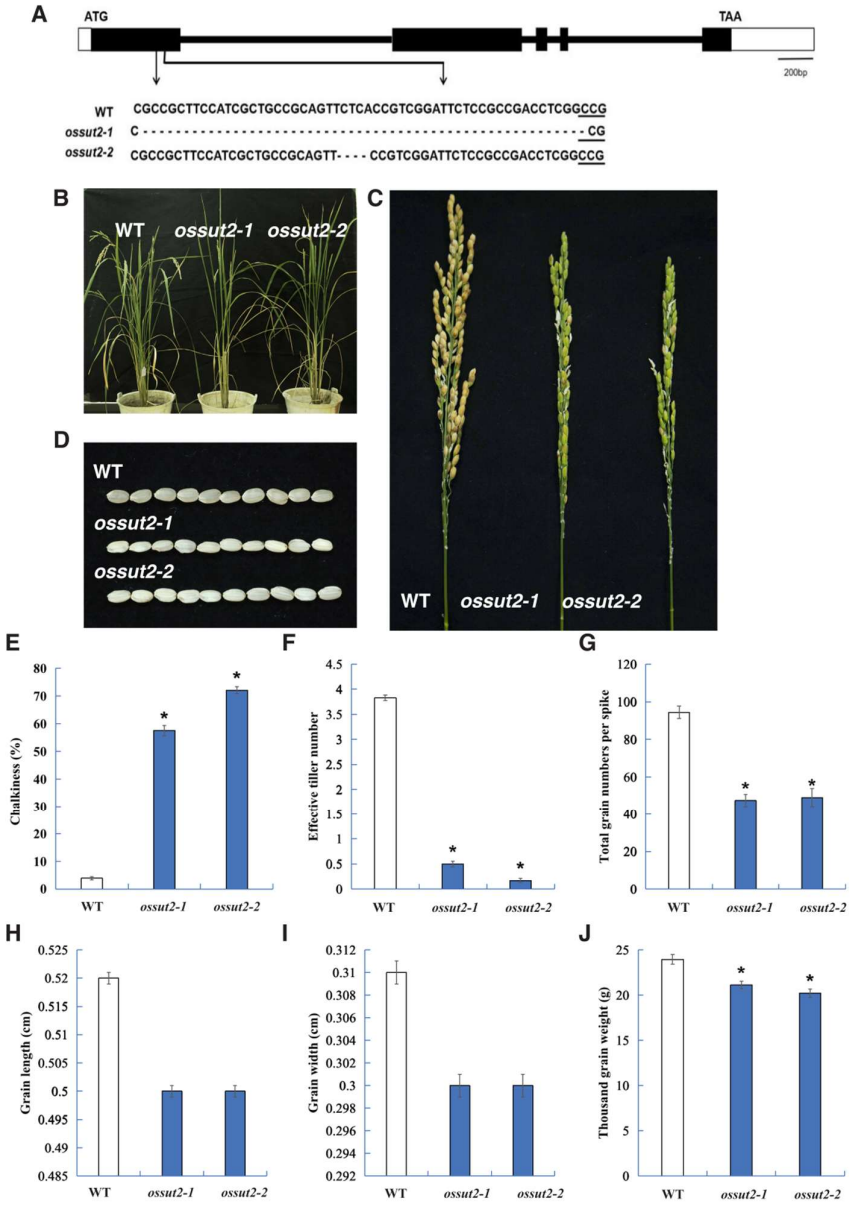

Figure 1. Identification of *OsSUT2* mutants. (A) Schematic diagram of the *OsSUT2* gene editing target site. Note: black regions represent the *OsSUT2* gene; black boxes indicate exons, black thick lines indicate introns, and black

 doi:10.20944/preprints202604.0166.v1

dashed lines indicate deleted nucleotide regions. ATG and TAA represent the start and stop codons, respectively. WT, wild type; mutants are designated *ossut2-1* and *ossut2-2*. (B-D) Comparison of plant morphology, panicle morphology and grain chalkiness between the WT and mutants.（E-J）Investigation of agronomic traits in the WT and mutants.

At the maturity stage, agronomic traits were measured in the WT and mutants. Compared with WT, the chalkiness degree of *ossut2-1* and *ossut2-2* was increased by 14.84-fold and 18.59-fold, respectively (Figure 1E). The number of effective tillers in the WT was approximately eightfold higher than that in *ossut2-1* and *ossut2-2*. The grain number per panicle of the two mutants was also significantly reduced. No significant differences were observed in grain length and grain width between the mutants and WT. The average 1000-grain weight was 23.94 g in the WT, but only 21.11 g in *ossut2-1* and 20.22 g in *ossut2-2*, indicating a significant decrease in 1000-grain weight of the mutants (Figure 1F–J).

3.1.2. Effect of OsSUT2 on the Accumulation of Endosperm Storage Substances

Starch is the major storage substance in rice endosperm and is metabolically interconvertible with glucose, sucrose, and fructose. Using three types of soluble sugars, total starch, Tre6P, amylose, and amylopectin as core detection indicators, we systematically analyzed changes in core carbon metabolism compounds in *ossut2* mutants at three developmental stages: 6-week-old leaves (source organ, vegetative stage), grains at 20 days after flowering (sink organ, key grain-filling stage), and mature endosperm (sink organ, final filling stage), clarifying the metabolic basis for this gene's regulation of grain chalkiness.

Leaves of 6-week-old *ossut2-1*, *ossut2-2* and WT plants were collected, and the contents of sucrose, fructose, glucose and total starch were determined. Compared with the WT, the levels of fructose, glucose, sucrose and total starch were significantly increased by approximately one-fold in the mutant leaves (Figure 2A-D), which were largely consistent with those reported by Eom et al.[6], suggesting that mutation of *OsSUT2* caused abnormal sugar accumulation in rice leaves and disturbed sugar transport in plant. The increased soluble sugars and total starch in the mutants resulted from blocked sugar transport from source leaves to sink grains, which impaired the conversion of fructose and glucose to sucrose and inhibited starch degradation, thereby reducing the precursors required for starch synthesis in sink grains [23].

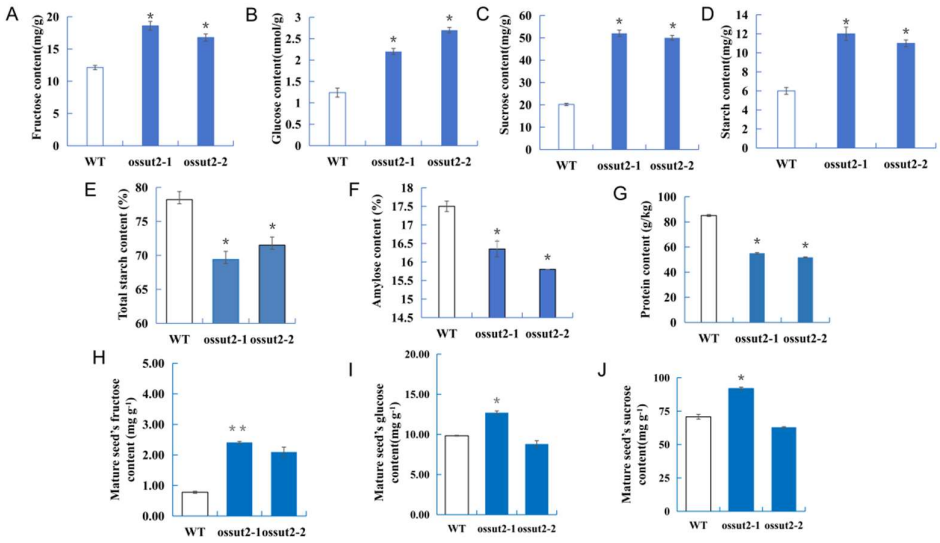

Figure 2. Changes in soluble sugar and total starch contents in *ossut2-1* and *ossut2-2* mutants. (A–D) Contents of soluble sugars (fructose, glucose, sucrose) and total starch in leaves of wild-type and mutant plants at 6 weeks

 doi:10.20944/preprints202604.0166.v1

of age; (E–G) Contents of total starch, amylose, and protein in mature grains of wild-type and mutant plants; (H–J) Contents of fructose, glucose, and sucrose in mature grains of wild-type and mutant plants.

Accumulation of storage substances and activities of starch metabolic enzymes were examined in endosperm of grains at 20 days after flowering. Compared with the wild type, amylose content was significantly decreased and amylopectin content was significantly increased in the mutants at 20 days after flowering, while no significant difference in total starch content was detected (Figure 3A). For sugar components, glucose and Tre6P contents were significantly decreased, fructose content significantly increased, and sucrose content unchanged obviously in mutant grains (Figure 3B–3C). Analysis of enzymes involved in amylopectin synthesis showed that DBE activity exhibited no significant difference, whereas SSS and SBE activities were significantly elevated, indicating enhanced chain elongation and branching of amylopectin in the mutants. For amylose synthesis, GBSS activity was significantly increased in mutant grains, but amylose content was still markedly reduced (Figure 3D–3G). In addition, α-amylase activity was significantly decreased in the mutants, suggesting that starch degradation was inhibited (Figure 3H). At maturity, total starch, amylose, sucrose, glucose, fructose, and protein contents were measured in grains of the WT and *ossut2-1*, *ossut2*-2 mutants. Total starch, amylose, and protein contents were significantly lower in the mutants than in the WT, whereas soluble sugar contents were significantly higher (Figure 2E-2J), indicating that the conversion from soluble sugars to starch was blocked in mature mutant seeds.

The above results indicated that the sugar transport process was significantly inhibited in the *ossut2-1* and *ossut2-2* mutant plants, with the contents of fructose, glucose, sucrose and total starch in the source leaves being nearly double those in the WT. The core reason was that the photoassimilated sucrose in leaves could not be transported to the grains in a timely manner, which led to the blockage of sugar conversion and starch degradation, and thus insufficient carbon precursors for starch synthesis in the sink organs [24]. At the key grain-filling stage, the amylose content in the endosperm of the mutants decreased significantly, while the amylopectin content increased markedly, which was associated with the increased activities of SSS and SBE, as well as the abnormal accumulation of amylose despite the elevated activity of GBSS. Meanwhile, the contents of glucose and Tre6P decreased, fructose content increased, and the reduced activity of α-amylase hindered starch degradation. These changes maintained the total starch content stable but caused an imbalance in starch components [6]. At the mature stage, the contents of total starch, amylose and protein in the endosperm of the mutants were reduced, whereas the soluble sugar content was increased, which further confirmed the blockage of soluble sugar-to-starch conversion and the abnormal accumulation of storage substances in the endosperm [24]. The impaired sugar transport in source organs induced the imbalance in starch synthesis and components in sink organs, which ultimately led to the failure of orderly deposition of endosperm starch granules, the destruction of amyloplast structure, the formation of voids in the endosperm and the reduction of transparency, thus resulting in a high chalkiness phenotype [25]. In addition, the sugar metabolism imbalance caused uneven nutrient distribution in the plants, leading to the inferior agronomic traits such as reduced tiller number and 1000-grain weight.

 doi:10.20944/preprints202604.0166.v1

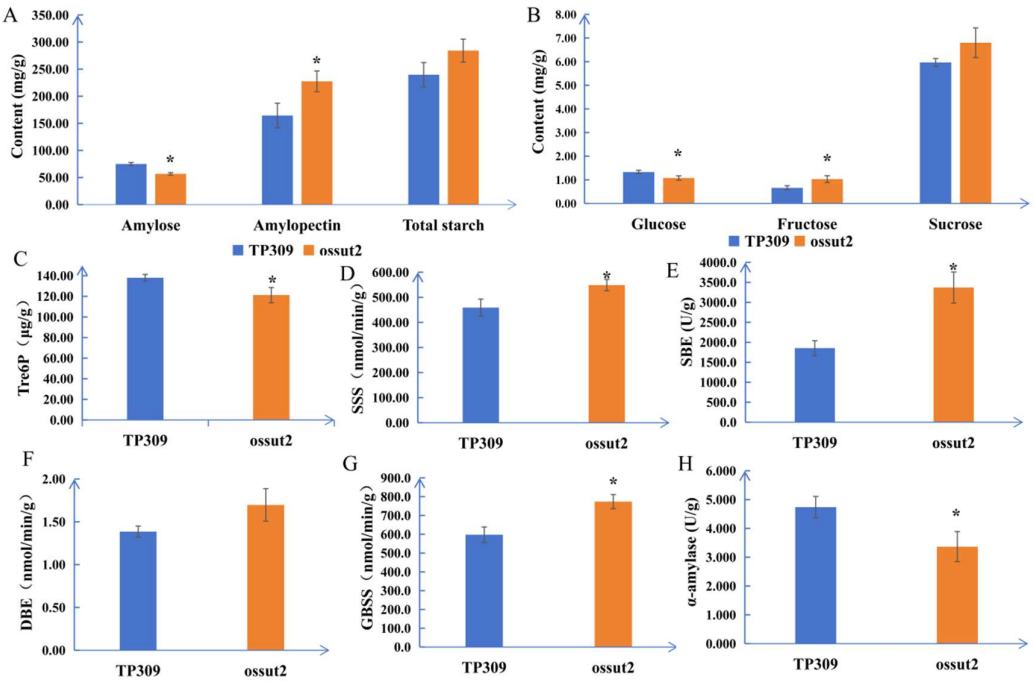

Figure 3. Differences in endosperm storage substances between wild-type TP309 and *ossut2* mutant grains at 20 days after flowering.

3.2. The Effect of OsSUT2 on the Fine Structure of Endosperm Starch

To investigate the effects of *OsSUT2* on starch fine structure, the crystal structures of the mutants and the WT were analyzed via XRD (Figure 4A). A single peak was detected at 15°2θ and 23°2θ, and a double peak at 17°2θ and 18°2θ in both the two mutants and the WT, all belonging to the A-type crystal pattern. No alteration was observed in the crystal pattern of the mutants, whereas a significant reduction in crystallinity was determined in the mutants compared with the WT, with *ossut2-1* exhibiting the lowest crystallinity, which indicated damage to the starch crystal structure in the mutants(Table 1). The FT-IR absorption curves were highly consistent, demonstrating that no obvious changes occurred in the basic chemical structure and short-range ordered configuration of starch between the mutants and the WT(Figure 4B). However, the 1045/1022 cm^{-1} absorbance ratio was significantly elevated in the mutants (Table 1), implying a relatively enhanced short-range order or molecular chain regularity of starch in the mutants. Meanwhile, the 1022/995 cm^{-1} ratio was markedly decreased (Table 1), which suggested a reduction in the intermolecular hydrogen bond strength of starch and a potential impact on the aggregation state of starch molecules. Analysis of starch chain-length distribution revealed no significant difference in the proportion of amylopectin short chains (AP1) between the WT and the mutants, while the proportion of the AP2 was significantly increased and the content of the AM was decreased in the mutants (Figure 4C).

Table 1. Crystallinity and FT-IR analysis results of the wild type and mutants.

Sample	Degree of crystallinity(%)	Crystal pattern	1045/1022	1022/995
WT	35.37^{a}	A	0.76^{c}	1.26^{a}
ossut2-1	31.35^{c}	A	0.78^{b}	1.18^{b}
ossut2-2	34.89^{b}	A	0.80^{a}	1.15^{b}

 doi:10.20944/preprints202604.0166.v1

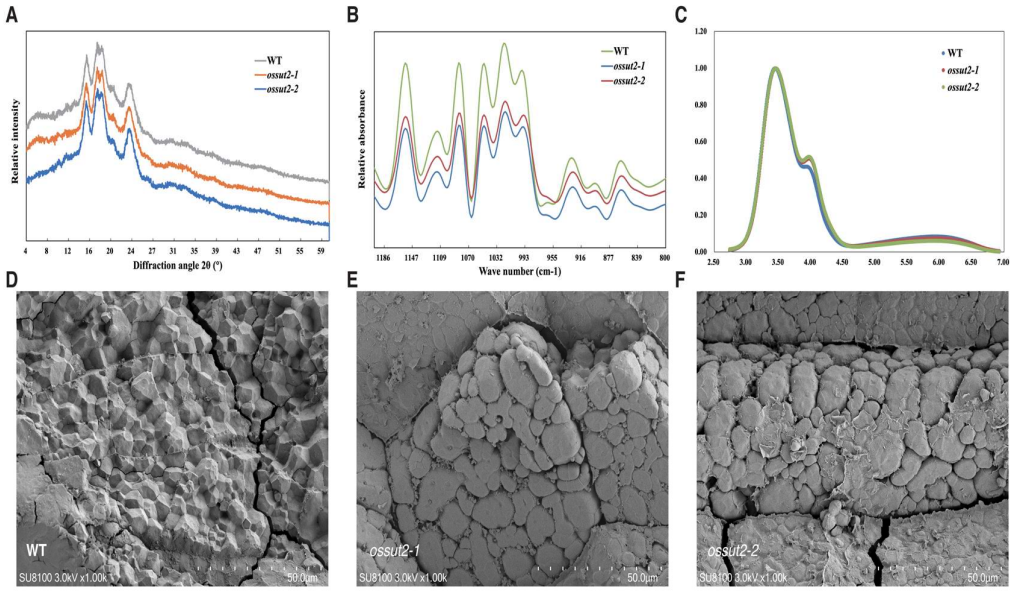

Figure 4. Fine structure of endosperm starch and transverse section characteristics of brown rice grains in the wild type and mutants. (A-C) XRD patterns, FT-IR spectra and starch chain-length distribution profiles; (D-F) SEM images of transverse sections of mature grains in the wild type and mutants.

Collectively, the above results indicated that loss of *OsSUT2* function induced specific alterations in starch structure, characterized by reduced crystallinity and elevated short-range order. These changes were likely associated with the modified starch chain-length distribution in the mutants, namely a significant increase in the proportion of the AP2 and a decrease in the AM content. The elevated AP2 proportion facilitated the local ordered stacking of double helices, whereas the reduced AM content impaired the stability of long-range crystalline structures [26]. Previous studies have demonstrated that decreased crystallinity is generally correlated with a higher starch digestion rate, and an increased AP2 proportion can alter the gelatinization temperature and cooked rice viscosity, which collectively determine the cooking, eating and nutritional quality of rice [27]. Thus, *OsSUT2* mediates the remodeling of endosperm starch from the level of chain-length distribution to multi-scale ordered structures through the regulation of sugar transport, thereby exerting a regulatory effect on rice quality.

To elucidate the cytological mechanism underlying chalkiness formation in the mutants, the transverse sections of endosperm from mature seeds of the WT and *ossut2* mutants were observed via SEM. It was found that starch granules in the chalky regions of *ossut2* mutants exhibited uneven size, irregular morphology, loose arrangement and enlarged intergranular spaces, whereas those of the WT were uniform in size, regular in morphology and densely arranged (Figure 4D-F). These results indicated that *OsSUT2* mutation alters the morphology and spatial arrangement of endosperm storage substances, thereby exacerbating grain chalkiness [28].

3.3. Identification of OsSUT2 Overexpression and Analysis of Its Tissue-Specific Expression Pattern

3.3.1. Generation and Characterization of OsSUT2 Overexpression Plants

To verify the chalky phenotype associated with *OsSUT2*, we constructed the pBWA(V)KS-*OsSUT2* overexpression vector and transformed it into the *ossut2* mutant background. A total of 21 transgenic lines were obtained, among which 12 were positive transgenic plants. Three PCR-positive transgenic lines (*OsSUT2-OE-1*, *OsSUT2-OE-2*, and *OsSUT2-OE-3*) were selected for further analysis. Using WT and *ossut2* mutant plants as controls, RT-qPCR was performed to quantify the relative expression level of *OsSUT2* in grains at 20 days after flowering in *OsSUT2* overexpression lines. The

 doi:10.20944/preprints202604.0166.v1

results showed that the expression level of *OsSUT2* was significantly lower in the *ossut2* mutant than in the wild type ($p < 0.01$). However, no significant difference was observed between the three overexpression lines and the wild type (Figure 5). The *OsSUT2-OE-2* showed the highest expression level, indicating that *OsSUT2* was efficiently and stably expressed and restored to wild-type levels in transgenic plants.

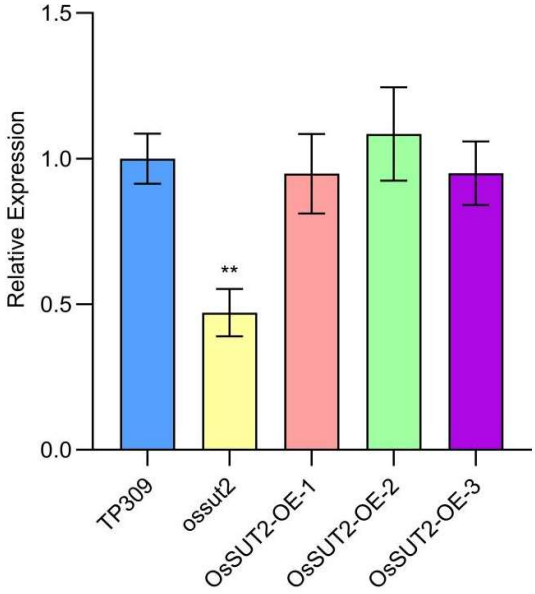

Figure 5. Expression analysis of *OsSUT2* in wild-type, mutant and overexpression lines.

After harvesting mature seeds, chalkiness-related traits were determined using a rice appearance quality analyzer. The results showed that the chalky grain rate and chalkiness degree were significantly higher in the *ossut2-1* (32%, 15.9%) and *ossut2-2* (38%, 23.6%) mutants than in the WT (12%, 8.6%). In contrast, these two traits were markedly decreased in the three overexpression lines (chalky grain rate: 9%–15%; chalkiness degree: 7.8%–9.9%), with no significant difference from the WT ($p > 0.05$), indicating that the chalky phenotype was fully restored (Figure 6).

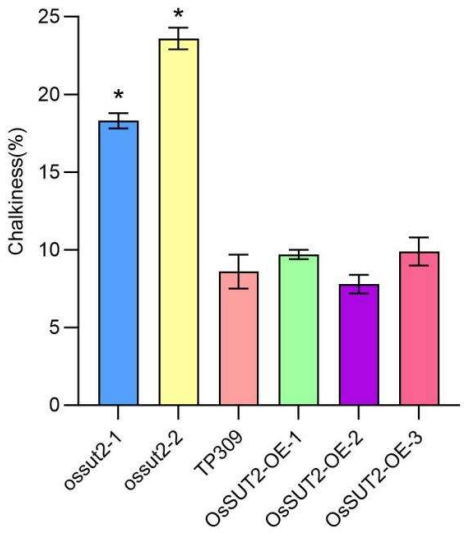

Figure 6. Chalkiness degree in wild-type, mutant, and overexpression lines.

 doi:10.20944/preprints202604.0166.v1

3.3.2. Analysis of the Tissue-Specific Expression of OsSUT2

To characterize the tissue-specific expression profile of *OsSUT2* in rice, qRT-PCR analysis was performed on the leaves, stems, sheaths, and panicles of wild-type TP309 and *ossut2* mutant lines. The results showed that compared with the WT, the expression level of *OsSUT2* in all detected tissues of the *ossut2* mutants was significantly reduced, and the down-regulation range varied among different tissues: the most significant decrease was observed in panicles, where the expression levels of the two mutants were almost close to zero; the expression levels in leaves, stems, and leaf sheaths were also down-regulated to varying degrees (Figure 7).

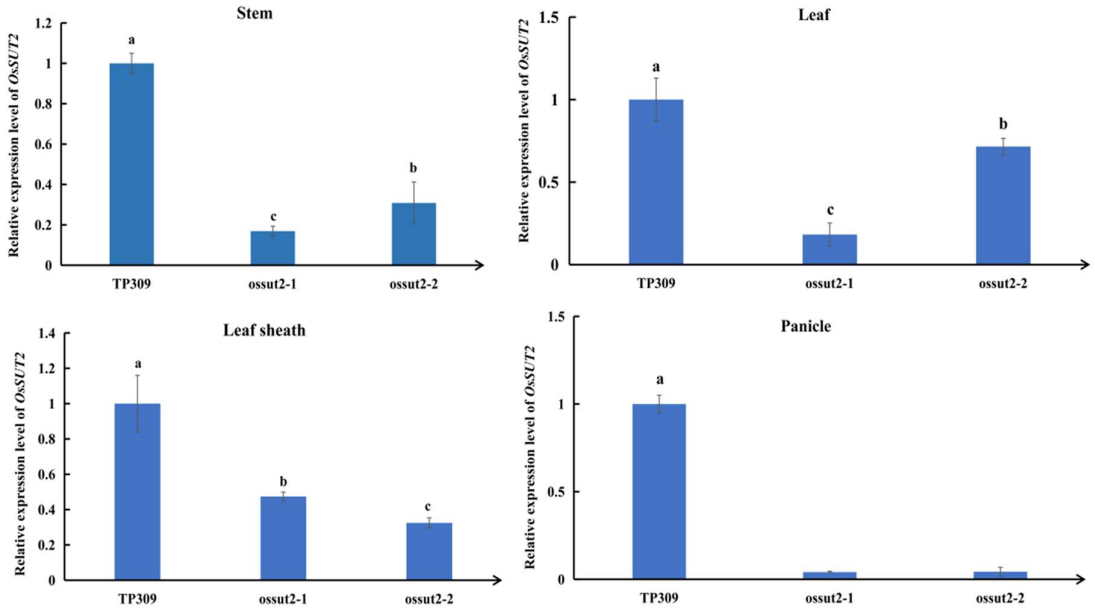

Figure 7. Expression analysis of *OsSUT2* in different tissues.

These results indicated that *OsSUT2* was expressed in both source and sink organs of rice, and the loss of its function exerted the most significant transcriptional repression effect on panicles. This suggested that *OsSUT2* might play a more critical role in grains during the grain filling stage than in leaves during the vegetative growth stage, which might explain why the mutation of this gene led to abnormal endosperm starch structure, more significant chalkiness, and worse agronomic traits.

3.4. Transcriptome Analysis of the Ossut2 Mutant and WT

3.4.1. Differences in Transcriptome Expression Patterns and Validation of Reproducibilit

To evaluate the overall expression differences in the endosperm transcriptomes between the *ossut2* mutant (KO, ST3) and the wild type (WT, TP309), transcriptome sequencing was performed on grains at 20 days after flowering, with 3 biological replicates per group. PCA showed that the correlation coefficients between biological replicates within each group were all greater than 0.925, which were significantly higher than those between groups, indicating good intra-group reproducibility (Figure 8). PCA revealed that the KO and WT samples were clearly separated along the first principal component (PC1, explaining 76.60% of the variation), while samples within each group were closely clustered. This suggested that the mutation of *OsSUT2* led to significant changes in the overall gene expression pattern of rice endosperm, and the experimental data were highly reliable and reproducible (Figure 9). The boxplot of gene expression distribution showed that the $\log_2$(FPKM + 1) distributions of samples within and between WT and KO groups were consistent,

 doi:10.20944/preprints202604.0166.v1

with a median between 2 and 3, indicating accurate quantification of sequencing data and no obvious batch effect (Figure 9).

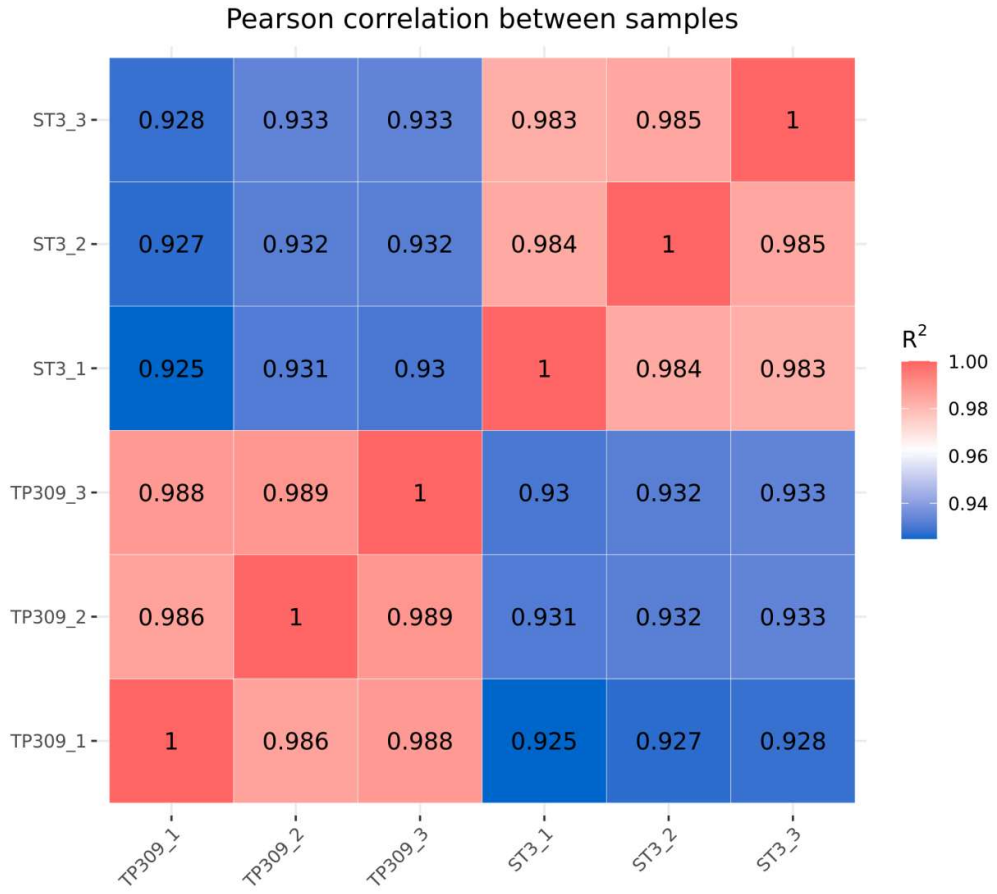

Figure 8. Sample correlation heatmap.

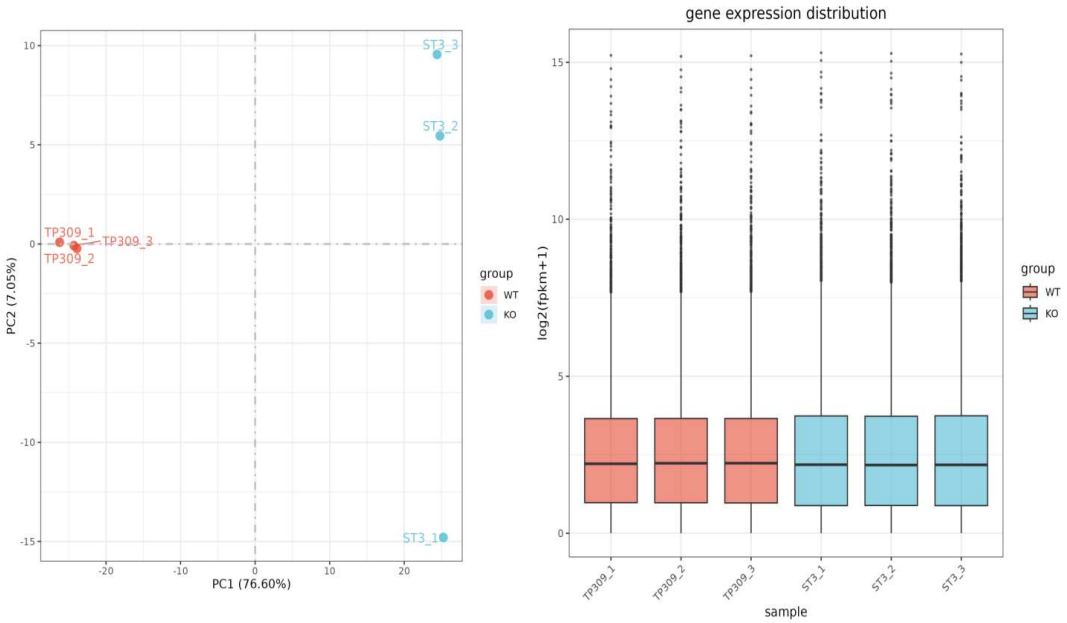

Figure 9. PCA plot of transcriptome samples on the left, and boxplot of gene expression on the right.

 doi:10.20944/preprints202604.0166.v1

3.4.2. Differentially Expressed Genes (DEGs)

3.4.2.1. Analysis of DEGs Between the WT and Ossut2 Mutant

Venn diagram analysis identified 19,293 expressed genes in the WT and KO groups, of which 16,810 were co-expressed, 1,477 were exclusive to the WT, and 1,006 to the KO. These results indicated that *OsSUT2* mutation altered the expression levels of existing genes and induced the specific expression of some genes (Figure S1). Based on volcano plots, a total of 5158 DEGs ($|\log_2FC| > 1$, padj < 0.05) were identified in the transcriptomic comparison of endosperm between *ossut2* mutant and WT, among which 2337 were up-regulated and 2821 were down-regulated (Figure 10). Furthermore, focusing on key pathways including sucrose transport, sucrose synthesis and starch metabolism, 15 crucial differentially expressed genes were characterized (Table S1, Figure 11). Their expression patterns were highly consistent with the carbon metabolic disorder caused by the loss of *OsSUT2* function, providing an important basis for dissecting the molecular mechanism underlying the chalky phenotype.

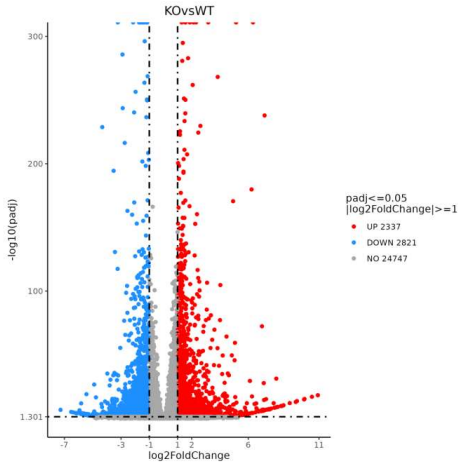

Figure 10. Volcano plot of DEGs.

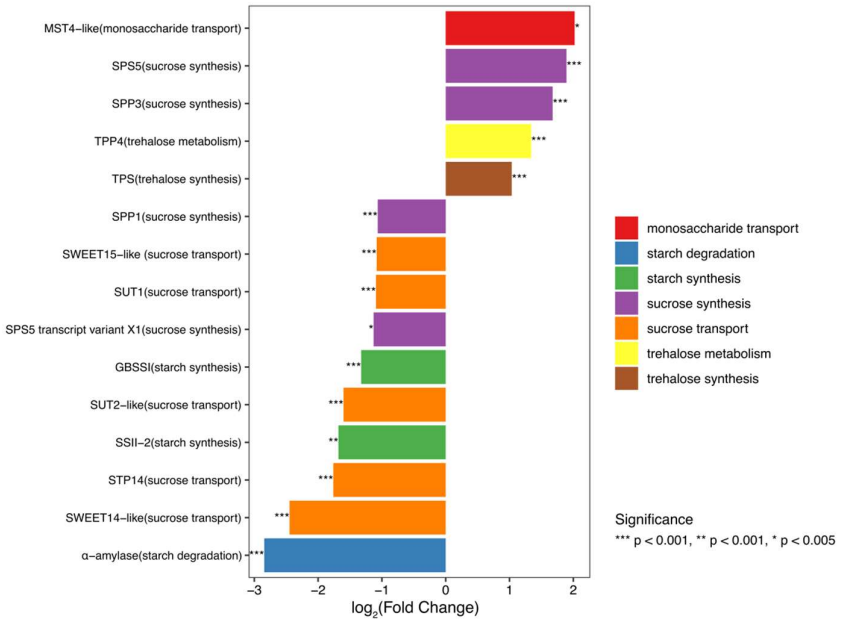

Figure 11. Differentially expressed genes related to sugar transport and starch synthesis pathways.

 doi:10.20944/preprints202604.0166.v1

As shown in Figure 11, mutation of *OsSUT2* resulted in systematic obstruction of the sucrose transport pathway in endosperm. Key genes involved in long-distance and intercellular sucrose transport (*SUT2-like*, *SUT1*, *SWEET14-like*, *SWEET15-like*, *STP14*) were extremely significantly down-regulated, whereas the monosaccharide transporter gene *MST4-like* was significantly up-regulated, forming a compensatory regulation to maintain substrate supply for starch synthesis. The sucrose synthesis pathway showed a divergent pattern of "compensatory up-regulation and basal synthesis down-regulation". Stress-responsive synthase genes *SPS5* and *SPP3* were extremely significantly up-regulated to compensate for carbon source deficiency, while the basal synthase gene *SPP1* and several *SPS5* transcripts were significantly down-regulated. Core enzyme genes in the starch synthesis pathway (GBSSI, SSII-2) were comprehensively significantly down-regulated, directly demonstrating that starch synthesis capacity was markedly reduced due to insufficient carbon supply, providing direct molecular evidence for chalky phenotype formation. In addition, trehalose signaling pathway genes *TPS9* and *TPP4* were extremely significantly up-regulated in response to carbon metabolic stress, whereas α-amylase, a key enzyme for starch degradation, was extremely significantly down-regulated. This reduced carbon source loss by inhibiting starch degradation, forming a compensatory strategy to maintain starch accumulation.

Taken together, differential expression of core genes in the sucrose transport-sucrose synthesis-starch metabolism pathway in *ossut2* mutant endosperm caused a systematic carbon metabolism disorder ("impaired transport → synthetic divergence → attenuated starch synthesis → enhanced signal regulation"), providing direct evidence for the molecular mechanism of endosperm chalkiness induced by *OsSUT2* loss-of-function.

3.4.2.2. Heatmap of Expression Patterns for DEGs

Unsupervised clustering analysis was performed on DEGs in the endosperm of *ossut2* (KO) mutants and WT plants. In the heatmap (Figure 12), each row represented a DEG, and each column represented a biological replicate sample (TP309_1/2/3 for WT, ST3_1/2/3 for KO). The color gradient from blue to red indicated the change in gene expression level from low to high. The top dendrogram revealed that WT and mutant samples were clustered into distinct groups, demonstrating significant differences between the two groups. The clustering tree divided DEGs into two major modules: the upper module contained downregulated genes (with higher expression in WT but lower expression in mutants relative to WT), which were mainly enriched in sucrose transport and starch synthesis pathways; the lower module comprised upregulated genes (with higher expression in mutants relative to WT), which were primarily involved in compensatory sucrose synthesis and trehalose signaling regulation. This heatmap clearly illustrated the global transcriptomic remodeling triggered by *OsSUT2* mutation, laying a foundation for subsequent functional enrichment analysis and mechanistic studies.

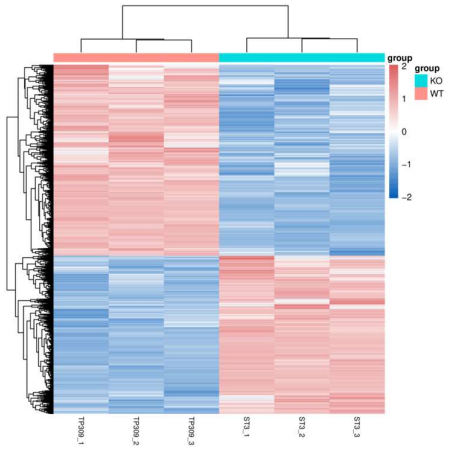

Figure 12. Heatmap of DEG expression patterns.

 doi:10.20944/preprints202604.0166.v1

3.4.3. GO and KEGG Enrichment Analysis

GO enrichment bubble chart analysis revealed the functional bias of DEGs between the *ossut2* mutant and WT (Figure 13A). Genes associated with carbohydrate metabolism and biosynthetic processes were significantly enriched in the mutant, which was highly consistent with the core physiological basis of chalkiness formation—abnormal starch synthesis and accumulation. Regarding molecular function, the significant enrichment of genes related to hydrolase activity acting on glycosyl bonds further confirmed that the loss of sugar transporter function directly disrupted sugar homeostasis in the endosperm. Meanwhile, the protein translation pathway contained the largest number of DEGs, and terms such as intracellular membrane-bounded organelles showed relatively high enrichment levels, suggesting that mutation of *OsSUT2* not only affected sugar metabolism but also indirectly regulated endosperm development by modulating the expression of genes related to protein synthesis and cell structure. Therefore, transcriptome enrichment analysis demonstrated that as a key sugar transporter, the functional deficiency of *OsSUT2* led to the formation of endosperm chalkiness in rice through the coordinated regulation of multiple pathways.

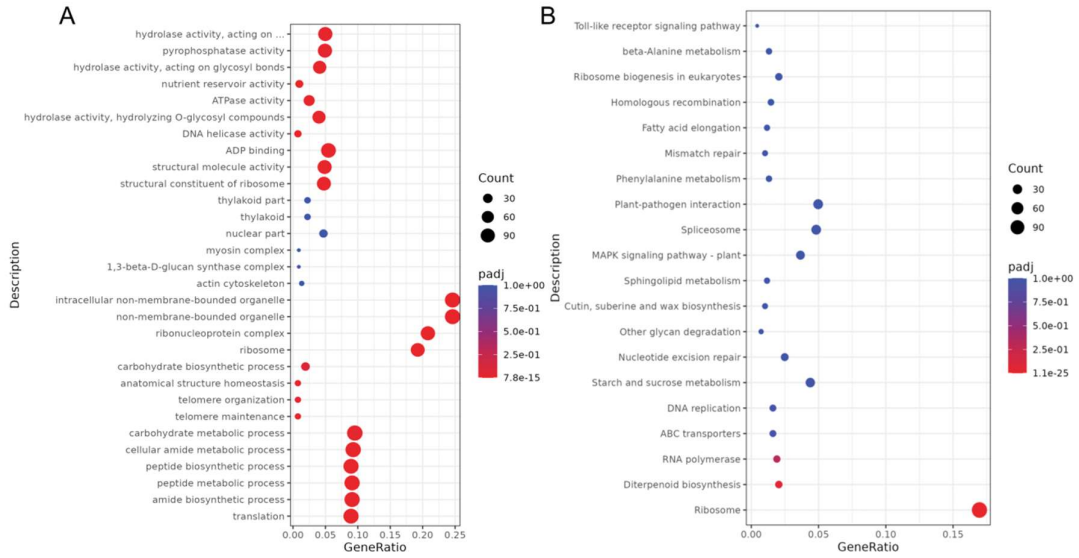

Figure 13. GO enrichment (A) and KEGG enrichment (B) of DEGs.

KEGG pathway enrichment analysis was performed on DEGs between the *ossut2* mutant and WT (Figure 13B and Figure S2). Only the ribosome pathway was significantly enriched among all detected pathways (padj = 1.106×10^{-25}), which contained 116 DEGs and represented the most severely disturbed core pathway in the mutant. Notably, the starch and sucrose metabolism pathway, which is directly associated with endosperm chalkiness formation, was not significantly enriched (padj = 0.990). However, this pathway included 30 DEGs, among which 20 (66.7%) were down-regulated, indicating an overall inhibitory tendency in the mutant. Combined with GeneRatio analysis (4.4% vs. background 3.3%), genes in this pathway were perturbed more frequently than random levels. These results further confirmed that mutation of *OsSUT2* directly disturbed sugar transport and metabolic homeostasis in the endosperm by repressing the starch and sucrose metabolism pathway, which represents one of the key molecular mechanisms underlying chalky phenotype formation.

Collectively, mutation of *OsSUT2* triggered global remodeling of the endosperm transcriptome. This was essentially attributed to the combined effects of repression of core pathways and compensatory regulation under disrupted carbon metabolic homeostasis, representing the core molecular logic underlying chalkiness formation. Loss of function of this gene directly downregulated key genes involved in sucrose transport and suppressed the expression of core enzyme genes for starch synthesis, leading to insufficient carbon supply and markedly reduced starch

 doi:10.20944/preprints202604.0166.v1

synthesis capacity in the endosperm, which was identified as the direct cause of chalkiness formation [24]. Meanwhile, plant cells initiated compensatory regulatory mechanisms to alleviate carbon metabolic disturbance: genes related to monosaccharide transport, stress-responsive sucrose synthases, and the trehalose signaling pathway were upregulated, whereas starch degradation genes were downregulated to reduce carbon loss. However, such compensatory regulation failed to reverse the functional defects of core pathways, ultimately resulting in imbalanced starch metabolism in the endosperm. Furthermore, *OsSUT2* mutation significantly disturbed pathways associated with ribosomes and protein translation, impairing the synthesis of functional proteins and the development of subcellular structures in endosperm cells. Acting synergistically with carbon metabolic disorders, these effects further exacerbated the phenotypic characteristics of loosely arranged and structurally damaged starch granules in the endosperm [25]. The present study confirmed at the transcriptomic level that *OsSUT2* was not only a critical protein mediating transmembrane transport of carbon assimilates between source and sink tissues, but also a central hub regulating endosperm carbon metabolism. By coordinately modulating multiple pathways during endosperm development, these findings refined the molecular regulatory mechanism of rice chalkiness formation at the level of sugar transport.

3.5. Haplotype Analysis of OsSUT2

To investigate the natural genetic diversity of the *OsSUT2* gene, haplotype distribution patterns in its coding region and flanking sequences were analyzed using 6048 accessions from the RiceAtlas database (http://60.30.67.242:18076/#/home)[22]. Three major haplotypes (Hap1, Hap2, and Hap3), composed of nine SNP loci, were identified, with significant indica-japonica differentiation in their distribution (Table S2, Figure 14).

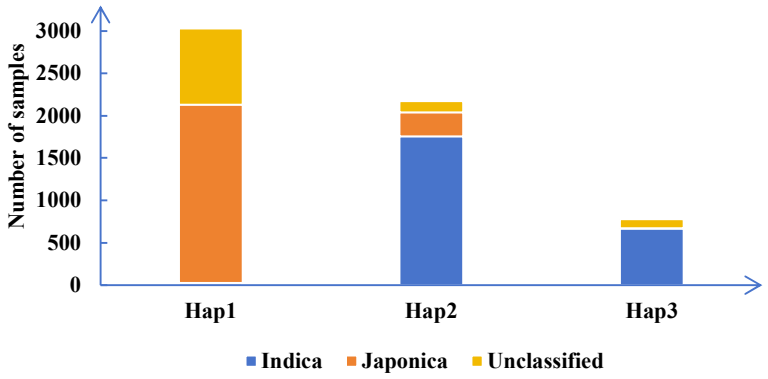

Figure 14. Haplotype analysis of *OsSUT2*.

Hap1 was a japonica-specific haplotype, with 3028 valid accessions, predominantly enriched in major japonica-growing regions including Northeast China, North China, and Central China japonica areas. In contrast, Hap2 and Hap3 were indica-enriched: Hap2 (2173 valid accessions) was mainly distributed in major indica-producing regions (Central China, Southwest China) with a small presence in japonica regions, while Hap3 (776 valid accessions) exhibited a stronger indica-specificity, with only negligible frequencies in japonica regions.

These results demonstrated that haplotype differentiation of *OsSUT2* was closely associated with the genetic divergence between indica and japonica subspecies, indicating adaptive selection of this gene during the evolutionary divergence of indica and japonica rice.

 doi:10.20944/preprints202604.0166.v1

4. Conclusion

In this study, homozygous mutants *ossut2-1* and *ossut2-2* were generated from rice TP309 using the CRISPR/Cas9 technology. Combined with multiple technical approaches including overexpression verification, phenotypic characterization, endosperm storage substance analysis, cytological observation, and transcriptome sequencing, the molecular mechanism by which *OsSUT2* regulates rice chalkiness formation was systematically elucidated.

Loss of *OsSUT2* function was found to significantly increase the chalkiness degree and deteriorate agronomic traits such as effective tiller number and 1000-grain weight. Massive accumulation of carbon assimilates in source organs and impairment of sugar transport and starch synthesis in sink organs were caused by the loss of this gene, leading to imbalanced source-sink transport. Loosely arranged endosperm starch granules, decreased crystallinity, and damaged fine structure were confirmed as the core cytological causes of chalkiness. *OsSUT2* was expressed in both source and sink organs of rice, with the most significant suppression in panicles. Transcriptome sequencing showed that *OsSUT2* mutation triggered systematic disorders in sucrose transport, synthesis, and starch metabolism pathways in endosperm. These metabolic disorders were reversed by overexpression of *OsSUT2*, which restored normal starch granule morphology and eliminated chalkiness, confirming that *OsSUT2* is a key gene regulating rice chalkiness. Three major haplotypes of *OsSUT2* were identified by haplotype analysis, with obvious indica-japonica differentiation, providing a natural variation basis for molecular marker development.

This study clarifies that *OsSUT2* regulates chalkiness formation by mediating source-sink carbon assimilate transport, controlling starch metabolism and starch fine structure, and provides important gene resources and molecular marker basis for genetic improvement of rice chalkiness.

Supplementary Materials: The following supporting information can be downloaded at the website of this paper posted on Preprints.org, Figure S1: Venn diagram of transcriptome sequencing between wild-type (WT) and knockout (KO) mutants; Figure S2: KEGG enrichment bar chart of DEGs; Table S1: DEGs related to sugar transport and starch synthesis; Table S2: Haplotype analysis of the *OsSUT2* gene.

Author Contributions: Conceptualization, Dongping Yao, Xiaoqiao Yin and Bin Bai; Methodology, Dongping Yao, Xiaoqiao Yin, Dengkui Liu, Fudie Meng, Chunfen Long, Yingge Li, Xuemei Zhong and Bin Bai; Formal analysis, Dongping Yao, Dengkui Liu, Fudie Meng, Chunfen Long, Yingge Li and Xuemei Zhong; Investigation, Dongping Yao, Xiaoqiao Yin, Chunfen Long, Yingge Li and Xuemei Zhong; Resources, Xiaoqiao Yin, Dengkui Liu and Fudie Meng; Writing – original draft, Dongping Yao; Writing – review & editing, Bin Bai; Visualization, Dongping Yao; Supervision, Bin Bai; Project administration, Bin Bai; Funding acquisition, Bin Bai. All authors have read and agreed to the published version of the manuscript.

Funding: This research was financially supported by the Inter-departmental Joint Fund of Hunan Provincial Natural Science Foundation (2025JJ80298), the National Natural Science Foundation of China (No. 32201884), the scientific research project from the Department of Education of Hunan Province, China (25C1261).

Data Availability Statement: The original contributions presented in this study are included in the article/supplementary material. Further inquiries can be directed to the corresponding author(s).

Conflicts of Interest: The authors declare no conflict of interest.

References

1. Wing, R.; Purugganan, M.; Zhang, Q. The rice genome revolution: from an ancient grain to Green Super Rice [J]. *Nature Reviews Genetics* **2018**, 19, 505-517.
2. Zhao, D.; Zhang, C.; Li, Q.; Liu, Q. Genetic control of grain appearance quality in rice [J]. *Biotechnology Advances* **2022**, 60,108014-108014.
3. Ji, J.; Yang, L.; Fang, Z.; Zhang, Y.; Zhuang, M.; Lv, H.; Wang, Y. Plant SWEET family of sugar transporters: structure, evolution and biological functions [J]. *Biomolecules* **2022**, 12, 205.

 doi:10.20944/preprints202604.0166.v1

4. Aoki, N.; Hirose, T.; Scofield, G.; Whitfeld, P.; Furbank, R. The sucrose transporter gene family in rice [J]. *Plant and Cell Physiology* **2003**, 44, 223-232.
5. Hirose, T.; Zhang, Z.; Miyao, A.; Hirochika, H.; Ohsugi, R.; Terao, T. Disruption of a gene for rice sucrose transporter, OsSUT1, impairs pollen function but pollen maturation is unaffected[J]. *Journal of Experimental Botany* **2010**, 6, 3639-3646.
6. Eom, J.; Cho, J.; Reinders, A.; Lee, S.; Yoo, Y.; ... & Jeon, J. Impaired function of the tonoplast-localized sucrose transporter in rice, OsSUT2, limits the transport of vacuolar reserve sucrose and affects plant growth [J]. *Plant Physiology* **2011**, 157, 109-119.
7. Li, J.; He, S.; Guo, Y.; Zhang, Y.; Zhang, L.; ... & Sun, C. Research progress and application strategies of sugar transport mechanisms in rice [J]. *Frontiers in Plant Science* **2024**, 15, 1454615.
8. Sun, C.; Wang, Y.; Yang, X.;Tang, L.; Wan, C.; ... & Deng, X. MATE transporter GFD1 cooperates with sugar transporters, mediates carbohydrate partitioning, and controls grain filling duration, grain size and number in rice (*Oryza sativa L.*) [J]. *Plant Biotechnology Journal* **2023**, 21, 621-634.
9. Li, Y.; Fan, C.; Xing, Y.; Yun, P.; Luo, L.; Yan, B.; Pen, B.; ... & He, Y. Chalk5 encodes a vacuolar H+ -translocating pyrophosphatase influencing grain chalkiness in rice [J]. *Nature Genetics* **2014**, 46, 398-404.
10. Zhang, C.; Zhao, D.; Li, Q.; Gu,M.; Liu, Q. Progresses in research on functional analysis of key genes involving in rice grain quality [J]. *Scientia Agricultura Sinica* **2016**, 49, 4 267-4283.
11. Wu, B.; Yun, P.; Zhou, H.; Xia, Dou.; GU, Y. ... & He, Y. Natural variation in WHITE-CORE RATE 1 regulates redox homeostasis in rice endosperm to affect grain quality [J]. *The Plant Cell* **2022**, 34, 1912–1932
12. Bai, A.; Lu, X.; Li, D.;Li, J.;Liu, C. NF-YB1-regulated expression of sucrose transporters in aleurone facilitates sugar loading to rice endosperm [J]. *Cell Research* **2016**, 26, 384-388.
13. Fujita, N.; Yoshida, M.; Asakura, N.; Ohdan,T.; Miyao, A.; Hirochika, H.; Nakamura, Y. Function and characterization of starch synthase I using mutants in rice [J]. *Plant Physiology* **2006**, 140, 1070-1084.
14. Zhang, L.; Qi, y.; Wu, M.; Zhao, L.; Zhao, Z.; Lei, C.; Hao, Y. ... & Wan, J. Mitochondrion-targeted PENTATRICOPEPTIDE REPEAT5 is required for cis-splicing of nad4 intron 3 and endosperm development in rice [J]. *The Crop Journal* **2021**, 9, 282-296.
15. Cen, X.; Dong, H.; Jiang, X.; Zheng, X.; Duan, E.; ... & Wan, J. Natural variation in OsTPS8 confers differential regulation of chalkiness and seed vigor in indica and japonica rice [J]. *Nature Genetics*, **2025,** 58, 1-12.
16. Yao, D.; Wu, J.; Luo, Q.; Zhuang, W.;Xiao, G.;Lei,D.;Bai, B. Influence of high natural field temperature during grain filling stage on the morphological structure and physicochemical properties of rice (Oryza sativa L.) starch. [J]. *Food Chemistry* **2020**, 310,125817.
17. Yao, D.; Wu, J.; Luo, Q.; Zhang, D.; Zhuang, W.; Xiao, G.; Deng, Q.; Bai, B. Effects of salinity stress at reproductive growth stage on rice (*Oryza sativa L.*) composition, starch structure, and physicochemical properties [J]. *Frontiers in Nutrition* **2022,** 9, 926217-926217.
18. Cho,Y.; Kang, K.; Functional Analysis of Starch Metabolism in Plants [J]. *Plants* **2020**, 9, 1152-1152.
19. Abe, N.; Asai,H.; Yago, H.; Oitome, N.; Itoh, R.; Crofts, N.; Nakamura, Y.; Fujita, N. Relationships between starch synthase I and branching enzyme isozymes determined using double mutant rice lines [J]. *Bmc Plant Biology* **2014**, 14(1): 80.
20. Kong, X.; Zhu, P.; Sui, Z.; Bao, J. Physicochemical properties of starches from diverse rice cultivars varying in apparent amylose content and gelatinisation temperature combinations [J]. *Food Chemistry* **2015**, 172, 433-440..
21. Zhang, D.; Yao, D.; WU, J.; Luo, Q.; Shen, H.; HU, M.; Meng, F.; Zhang, Y.; Liu, X.; ... & Bai, B. Differences in cooking taste and physicochemical properties between compound nutritional rice and common rice [J]. *Frontiers in Nutrition* **2024**, 11,1435977-1435977.
22. Ma, X.; Wang, H.; Yan, S.; Zhou, C.; Zhou, K.; Zhang, Q.; ... & Han, L. Large-scale genomic and phenomic analyses of modern cultivars empower future rice breeding design [J]. *Molecular plant* **2025**, 18, 651-668.
23. Macneill, G.; Mehrpouyan, S.; Minow, S.; ... & Eme, M. Starch as a source, starch as a sink: the bifunctional role of starch in carbon allocation [J]. *Journal of Experimental Botany* **2017,** 68(16): 4433-4453.

 doi:10.20944/preprints202604.0166.v1

24. Duan, Y.; Li, X.; Wu, Y.; Jiao, G.; Ma, L.; Dong, N.; Chen, P.; Chen, P.; Li, X.; Cao, R.; Chen, T.; Hu, P.; Wei, X. Identification of Sucrose Transporter (SUT) Genes Regulating Rice Yield and Quality [J]. *Rice Science* **2025**, 32, 287-291.
25. Yu, S.; Lo, S.; Ho, T. Source–Sink Communication: Regulated by Hormone, Nutrient, and Stress Cross-Signaling [J]. *Trends in Plant Science* **2015**, 20.
26. Warren, F.; Michael, J.; Bernadine, M. Infrared spectroscopy as a tool to characterise starch ordered structure—a joint FTIR–ATR, NMR, XRD and DSC study [J]. *Carbohydrate Polymers* **2016**, 139, 35-42.
27. Nakamura,Y.; Sakurai, A.; Inaba, Yumiko.; Kimura, K.; Iwasawa, N.; Nagamine, T. The fine Structure of Amylopectin in Endosperm from Asian Cultivated Rice can be largely Classified into two Classes [J]. *Starch - Stärke* **2002**, 54, 117-131
28. Singh, N.; Sodhi, S.; Kaur. M; Saxena, K. Physico-chemical, morphological, thermal, cooking and textural properties of chalky and translucent rice kernels [J]. *Food Chemistry* **2003**, 82, 433-439.